Vol. 5, Issue. 3, 2018, ISSN 2349-0780

Design and Performance of Damping Network Design for LCL Filters Using Grid-Connected Inverters

[1]P. Saravana Kumar[*], [2]Dr.S. Sutha Padmanabhan,
Research scholar/EEE, Anna University, Chennai, saravanakumaruce@gmail.com.
Associate Professor/EEE, University College of engineering, Dindigul, suthapadmanabhan@gmail.com.

Abstract

Grid-connected inverters have wide application in the field of distributed generation and power quality. As the power level demanded by these applications increase, the work focuses on passive damping network design for LCL filters of grid-connected inverters. Passive damping is considered as it is simple and more reliable. The work explores a split-capacitor resistive-inductive (SC-RL) passive damping scheme for use in high power applications. A method for component selection for the SC-RL scheme that minimizes the power loss in the damping resistors while keeping the system well damped is proposed. Analytical results show the losses and quality factor to be in the range of 0.05-0.1% and 2.0-2.5 respectively, which are validated experimentally.

Keywords: LCL filer, Daming Network, DC-AC Inverter, Common Mode Voltage.

I.INTRODUCTION

The use of grid-connected inverters is on the increase both at the point of generation and utilization. On the generation end, they are used to integrate renewable sources of power with the ac grid. In all the above applications, it must be ensured that the switching frequency ripple injected into the grid by the grid-connected inverter is within limits specified by the grid standards. This requires a properly designed filter at the output of the inverter. Further, the grid-connected inverter is expected to witness common griddisturbances like voltage sags, voltage swells and the like. It should have controls that ensure its operation under these disturbances. In this regard, the grid-connected inverters are expected to have good control performance. Also, the required power handling capabilities of the grid-connected inverters has increased and stands at a few MWs in the present day. This has necessitated research on general issues related to grid-connected invertersand on specific issues related to their operation at high power levels. As more of these converters are put to use, the research is towards making these inverters more reliable.

II.NEED FOR LCL FILTER IN GRID-CONNECTED INVERTERS

For pulse-width modulated (PWM) inverters with high carrier frequency, the ripple predominantly has frequency components at and around the switching frequency (ωsw) and its multiples. Fig. 1.1 shows a typical voltage spectrum observed at the output terminals of a 3-phase 2-level grid-connected inverter. Considering switching frequencies of 2 kHz and above,

the voltage harmonics appear at the harmonic order of h > 35. Hence, from Table 2.1, it can be stated that all individual odd and even harmonic components should be limited to 0.3% and 0.075% of the fundamental rated current respectively and the TDD should be limited to 5%.Let us attempt to use a simple first order L filter to achieve the required individual harmonic limit for the spectrum shown in Fig. 1.1. Considering a 4-wire connection with the neutral connected to the dc bus mid-point, the predominant harmonic component is at h = 200. If the chosen filter limits the 200th harmonic component of current to within 0.075%, all the other individual harmonic components will surely be within the limits as the impedance offered by the filter to all other harmonic components would almost be the same or higher. For the 200th harmonic, design system of grid tied output value of filter design a part of the damping network.

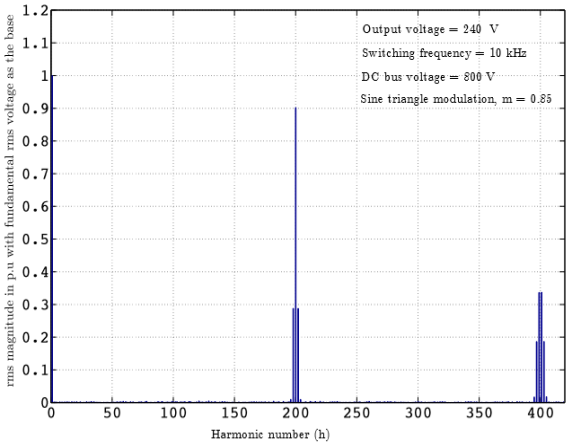

Figure 1.1: Harmonic spectrum of terminal voltage measured with respect to dc bus midpoint in a 3-phase 2-level inverter.

V (p.u) = 0.9 and I (p.u) = 0.00075 (as per limits). So, the required fundamental frequency impedance Z (p.u) is,

$$Z(p,u) = \omega(p,u).L(p,u) = \frac{V(p,u)}{I(p,u).200} = 6.\ \text{P.u.} \quad \text{---------- (1)}$$

The p.u impedance of 6.0 is too high. Besides being bulky and costly, the high filter impedance will increase the dc bus voltage requirement to impractical levels. The dc bus voltage is chosen such that the maximum ac voltage that can be produced at the output of the inverter will be able to balance the phasor sum of the grid voltage and the output filter drop. An increase in the switching frequency can be thought of as a solution to maintain the inductance value to be less and still maintaining the harmonic current limits. However, the increased switching losses and the limitations on the maximum switching frequency of the available devices will make it impossible. A higher order filter is the only viable solution. A second order LC filter is not usually opted as both the inverter considered and the grid are voltage sources and connecting a capacitor in parallel to a voltage source is redundant. Hence, a third order LCL filter is generally used. The next Section explains the LCL filter design.

III.LCL FILTER DESIGN

Fig. 1.2 shows the 3-phase 2-level inverter connected to the grid through a LCL filter. The 4-wire configuration gives the worst-case current ripple and is considered for the LCL filter design. The design outcome can be used for a 3-wire configuration also though it would be conservative. Discusses a method of choosing the ideal LCL filter components L1, L2 and C shown in Fig. 1.2. The design of the ideal LCL filter components used in this work follows a similar methodology.

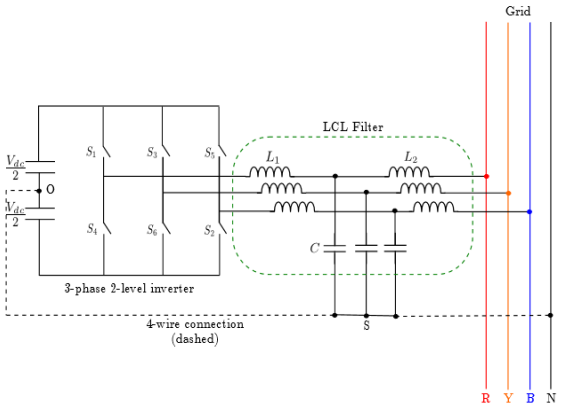

Figure 1.2: 3-phase 2-level inverter connected to the grid through a LCL filter in a 3-wire configuration (solid lines) and 4-wire configuration (dashed lines).

3.1 Choice of L

Fig. 1.3 shows the simplified circuit equivalent of the 4-wire configuration shown in Fig. 1.2. The grid is considered shorted for frequencies other than fundamental as the grid voltage is ideally zero at those frequencies. With the grid shorted and ωr representing the natural frequency of oscillation of an ideal LCL filter with no damping, it can be shown that,

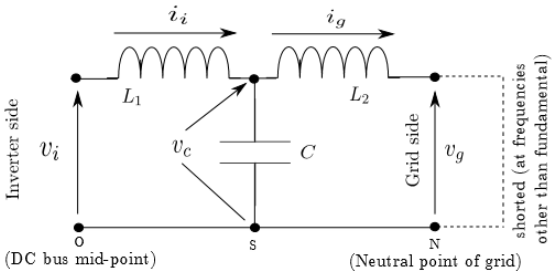

Figure 1.3: Per-phase circuit equivalent of the LCL filter connected between a 3-phase 2-level inverter and the grid in a 4-wire configuration.

The grid impedance is lumped along with L2.

$$\frac{I_g(s)}{V_i(s)} = \frac{1/L}{S[1+(S/wr)^2]} \qquad (2)$$

Where,

$$L = L_1 + L_2 \qquad (3)$$

$$w_r = \frac{1}{\sqrt{CL_p}} \qquad (4)$$

$$L_p = \frac{L_1 L_2}{L_1 + L_2} \qquad (5)$$

From equation (2)

$$L = \frac{|V_i(jw)|}{|I_g(jw)||jw||1-(w/w_r)^2|} \qquad (6)$$

Generally if the filter limits the dominant harmonic around the switching frequency to be within the individual harmonic limit, all other individual harmonics will also be within the limits. This can also be observed from Fig. 1.4, which shows a typical bode plot of Ig(s) /Vi(s) Considering considerably high switching frequencies of 2 kHz and above, the TDD will also be within the limits. If the dominant harmonic component is represented asw_{dom}, we have from (6),

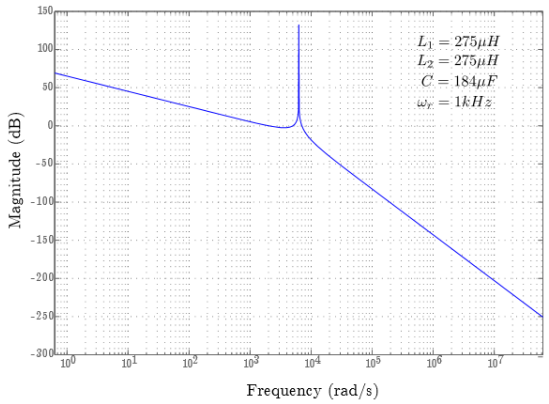

Figure 1.4: A typical body plot of the transfer functionIg(s)/ Vi(s) for an ideal LCL filter.

$$L_{min1} = \frac{|V_j(jw_{dom})|}{|I_g(jw_{dom})||jw_{dom}||1-(w_{dom}/w_r)^2|} \qquad (7)$$

Equation (7) gives a minimum value of L as any value of L lower than this will not meet the IEEE recommended harmonic limits. Consider a sample design where the choice of ωr is, ωr = 2·π·1000. On a frequency base of 2·π·50, ωr (p.u) = 20. The resonance frequency ωr sets the pass band frequency of the filter as can be observed from Fig. 1.4.

IV.COMPARISON OF DAMPING SCHEMES

Table 1.1 compares the power loss in the three mentioned damping schemes for the same damping level given by QF = 3.

A few points related to the comparison table are listed here:

• Pri is less in the case of SC-R damping as compared to R-damping as expected.

• Pfu is less in the case of SC-RL damping as compared to SC-R damping as expected.

• The value of |ig/vi|@f = fsw changes from that of the ideal LCL filter on addition of the damping components. The ideal value is -71 dB for the chosen LCL filter.The deviation from ideal value is more in the case of R damping as an additional zero getsadded into the system in R damping which changes the nature of the high frequency attenuation characteristics.

Parameter	**R Damping**	**SC-R Damping**	**SC-RL Damping**
fsw	9.75KHZ	9.75KHZ	9.75KHZ
fr	1KHZ	1KHZ	1KHZ
L1(p,u)	0.02	0.02	0.02
L2(p,u)	0.02	0.02	0.02
C(p,u)	0.25	-	-
C1(p,u)	-	0.125	0.125
Cd(p,u)	-	0.125	0.125
Rd(p,u)	0.0178	0.484	0.4
Ld(p,u)	-	-	0.0201
|ig/vi|@f = fsw	-59dB	-65dB	-65dB
QF	3.0	3.0	3.0
Pfu(%)	0.45	0.75	0.0016
Pri(%)	1.09	0.05	0.065
PT(%)	1.54	0.80	0.0666

Table 1.1: Comparison of R, SC-R and SC-RL damping schemes.

V.DAMPING DESIGN FOR LCL FILTER

Then, a detailed analysis of the Split-Capacitor Resistive-Inductive (SC-RL) scheme is presented. The better suitability of the SC-RL scheme as compared to the other schemes for use in high power inverters is shown. The hardware being of higher power, the SC-RL scheme is chosen. A novel component selection procedure is developed for the SC-RL passive damping scheme. The proposed method performs the design selection of the damping network components one at a time, optimizing the circuit parameters at each stage of addition of the components.

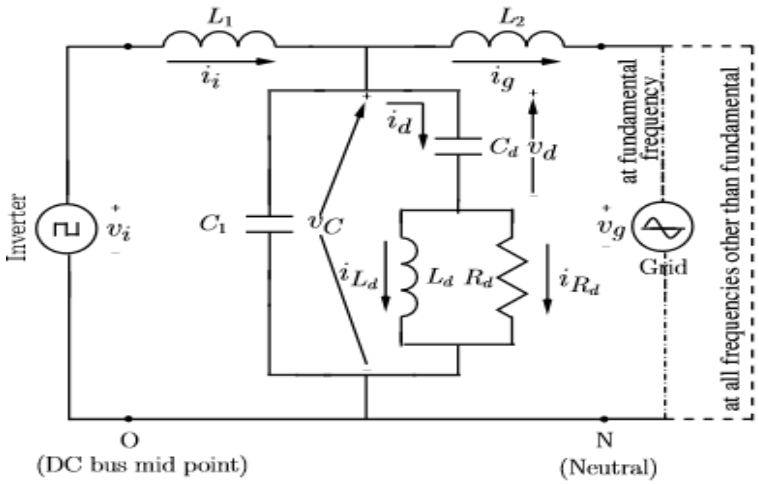

Figure 1.5: An SC-RL damped LCL filter at the output of one phase of a three-phase 4-wire inverter, showing the various state variables used to model the system.

5.1 Modeling of SC-RL Damped LCL Filter

The SC-RL damped LCL filter is modelled by considering one leg of a three-phase 4-wire inverter as shown in Fig. 2.8.

$$\frac{di}{dt} = \frac{1}{L1}V_i - \frac{1}{L1}V_c \quad (8)$$

$$\frac{di_g}{dt} = \frac{1}{L2}V_c - \frac{1}{L2}V_g \quad (9)$$

$$\frac{dv_c}{dt} = \frac{1}{C1}\left[i_1 - i_g - \left(iL_d + \frac{Vc-Vd}{Rd}\right)\right] \quad (10)$$

$$\frac{dv_d}{dt} = \frac{1}{C_d}\left[iL_d + \left(\frac{Vc-Vd}{Rd}\right)\right] \quad (11)$$

$$\frac{di_{Ld}}{dt} = \frac{1}{Ld}(Vc - Vd) \quad (12)$$

$$iR_d = \frac{1}{Rd}(Vc - Vd) \quad (13)$$

5.2 Quality Factor (QF)

VC(s)/Vi(s) – the capacitor voltage to inverter leg voltage, is the representative transfer function that is used to study the damping of the series resonance in the present work. Fig. 1.5 shows a typical plot of the transfer function VC(s)/Vi(s). The flat portion of the curve extends from dc to near resonance frequency. The nature of the bode plot explains the choice of the transfer function

VC(s)/Vi(s). The QF can be easily defined using this transfer function rather than for example, using the transfer function Ig(s)/Vi(s) shown for an ideal LCL filter.

Mathematically, the QF can be expressed as,

$$QF = \frac{\left|\frac{Vc(jw)}{Vi(jw)}\right| at\ w=wd}{\left|\frac{Vc(jw)}{Vi(jw)}\right| w\to 0} \qquad (14)$$

where, ωd is the resonance frequency of the LCL filter with the damping components included. ωd is that value of ω for which the magnitude of the transfer function peaks.

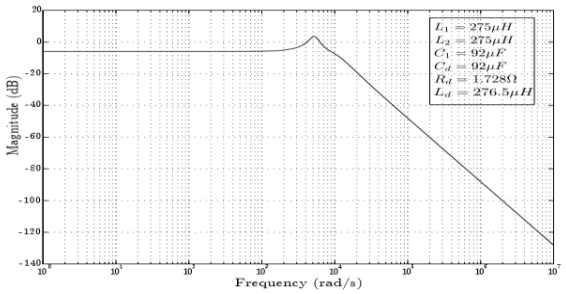

Figure 1.6: A typical body plot of the transfer function VC(s) Vi(s) for a SC-RL damped LCL filter.

5.3 Power Loss

The power loss primarily consists of two components - the fundamental frequency component, Pfu, and the switching ripple component, Pri. The switching frequency is well separated from the resonance frequency and does not excite any resonance component in steady state. However, in the hardware small resonance components that are excited by the transients and other sources such as switch non-idealities are usually observed. The QF being low, the current and hence the power loss due to this is negligible and is not considered for the total power loss (PT) computations. Loss due to fundamental frequency current: From Fig. 1.6 the fundamental power loss component, Pfu, in the damping resistor of the filter can be obtained as follows:

$$Pfu = R(Vc * Id)w = wfu \qquad (15)$$

$$Pfu = R\left\{\frac{VcVc^*}{\left[\frac{jwfuLdRd}{Rd+jwfuLd}+\frac{1}{jwfuCd}\right]^*}\right\} \qquad (16)$$

At fundamental frequency, the voltage magnitude at the inverter and the grid are close to 1 p.u. So, VC can be approximated to be 1 p.u as the voltage drop in the filter inductors L1and L2 is less. Substituting all quantities in per unit, we have,

$$Pfu = \frac{Cd^2Rd}{K^2Ld-2CdRdKLd+(1+C^2dR^2d)} \qquad (17)$$

The denominator function in represents a parabola with a symmetry parallel to the y-axis when KLd is plotted in the x-axis and the value of the function is plotted along the y-axis. Since the magnitude of a parabola increases rapidly with x-axis value, Pfu which is an inverse function falls to a low value quickly and changes very less there after the fundamental frequency power loss curve has a knee point as expected. After the knee point, the power loss almost remains a constant. So, any value of KLd after the knee point is a good choice from the perspective of Pfu.

VI.EXPERIMENTAL RESULTS

The experimental evaluation was carried out at an ac output voltage of 100 Vrms with a dc bus voltage of 400 V using the switching frequency used is 10 kHz. The various filter components used in the experimental validation are listed in Table 1.2. The table assumes the base values of power, voltage, current and frequency to be 2kVA, 240 V, 150mA and $(2\cdot\pi\cdot 50)$rad/s respectively. KLd was varied in the range 1 to 35 using series-parallel combinations of damping inductors. The various damping inductor values used and the equivalent KLd are listed in Table 1.3.

Parameter	L1=L2	C1=cd	Rd	Wr
Per unit value	0.05	0.032	1.24	25
Physical value	550uH	30uF	4.3Ω	2.π.1250 rad/s

Table 1.2: Filter component values used in the experimental set-up

Ld(uH)	400	520	975	1560	9000
KLd	34.2	26.3	14.0	8.8	1.5

Table 1.3: List of damping inductor values and equivalent damping impedance factor KLd used for measurements

6.1 Measurement of QF

A network analyzer (AP Instruments - Model 200) is used to experimentally determine the quality factors for various values of KLd. Fig.1.7 shows the theoretical and experimental quality factor curves.The deviations in the quality factor from the theoretical values can be attributed to the component tolerances and the non-idealities associated with the circuit elements. In particular, it can be observed that the experimental curve shows the damping to have improved over the theoretical prediction which is expected as the ESR of the inductor and capacitor and the wire resistances give additional damping.

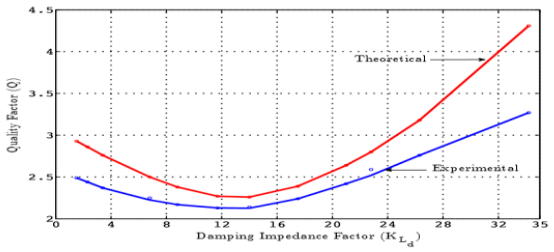

Figure 1.7: Theoretical and experimental quality factor curves as a function of the damping impedance factor KLd.

6.2 Measurement of Power Loss (Pfu and Pri)

To experimentally validate the fundamental frequency power loss Pfu in the filter damping resistor, the inverter should be connected to the grid through the SC-RL damped LCL filter. Equivalently, the current circulation procedure developed in system can also be used as only the fundamental frequency component of current in the damping resistor is of interest. Hence, the current circulation procedure is used in the present work. A digital power meter (Yokogawa - WT1600) is used to experimentally measure the power loss due to fundamental frequency component of current through the damping resistor (Rd). The worst case ripple current power loss is to be calculated at a duty ratio of d = 0.5. To experimentally validate the power loss in the damping resistor due to the worst case ripple current Pri, the grid is shorted i.e. the grid is disconnected and the grid-side inductors are connected to mid-point of the dc bus capacitor. Then, a 50% duty cycle pulse is applied at the output of the inverter and the loss due to the worst case ripple current in the damping resistor is measured using the data of current from high bandwidth LEM current sensors captured through LeCroy Wave Runner 6050 oscilloscope.

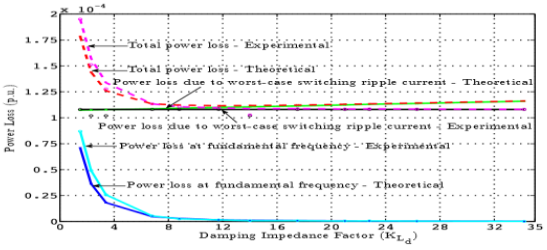

Figure 1.8: Theoretical and experimental power loss comparison as a function of the damping impedance factor KLd.

Fig.1.8 shows the theoretical and experimental power loss curves for fundamental component, ripple component and the total power loss. The experimental power loss curves closely match the values from the theoretical analysis for both fundamental and switching frequency components. As suggested in a selection of KLd = 12.5 based on (48) is a good choice in terms of QF and PT as observed from Fig.1.8and Fig. 1.9 respectively.

Quality	notation	Base value
Power	Pbase	40KVA

Voltage	Vbase	240V
Current	Ibase	55.6A
Impedance	Zbase	4.32Ω
Inductance	Ibase=Zbase/(2.π.50)	14mH
Capacitance	Cbase = 1/(2.π.50)	737uF
Frequency	Wbase	2.π.50 rad/s

Table 1.4: Base values used for the filter analysis.

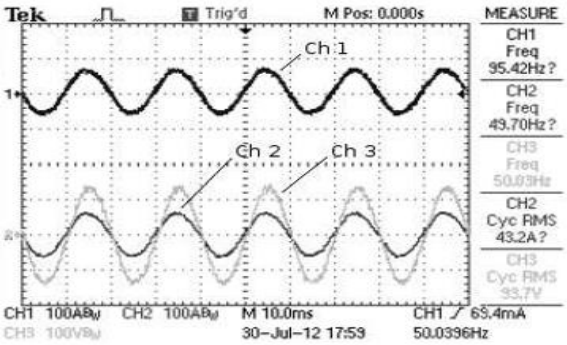

Figure 1.9: Operation of the inverter with LCL filter at an output of 100 V (rms), 40 A (rms) at unity power factor.

Fig. 2.1 shows the inverter-side inductor current, filtered grid-side inductor current and output filter capacitor voltage, VC. The waveform was captured with the inverter giving a sinusoidal output of 100V rms at unity power factor and carrying a line current of 40A. The damping inductor used was 390µH.

6.3 Filtering Performance

parameter	**Per unit value**	**Physical value**
L1=L2	0.02	275uH
C1=Cd	0.125	92uF
Rd	0.4	1.728Ω
wr	20	6283rad/s
wsw	195	61261rad/s

Table 1.5: Filter Parameter Values for SC-R Passive Damping.

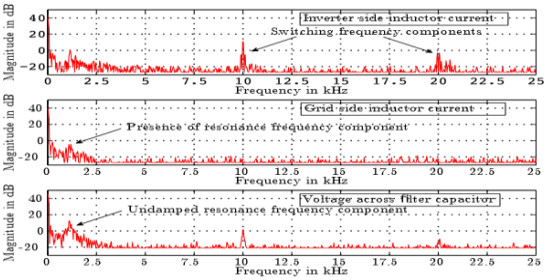

Fig2.1: Spectrum of waveforms

Fig. 2.1 show the inverter-side inductor current, filtered grid-side inductor current and output filter capacitor voltage without and with thewaveforms have been captured with the inverter giving a sinusoidal output of 100 V and unity power factor at the inverter output terminals. The line current is 40 A. In the case of damped LCL filter, the damping inductor used was 1.17 mH. the FFT spectrums show the filtering performance of the LCL filter and the effect of the passive damping circuitry at the resonance frequency. With damping, the grid side current ripple is 0.085 A and the inverter side current ripple is 4.01 A at the switching frequency. The corresponding filter attenuation (ig/vi) at the switching frequency is -64.25 dB. The experimentally obtained attenuation is close to the analytically computed attenuation of -66.8 dB. The capacitor voltage has oscillations of magnitude 2.58 V at the resonance frequency without damping. With the SC-RL damping network, the magnitude is reduced to 0.28 V.

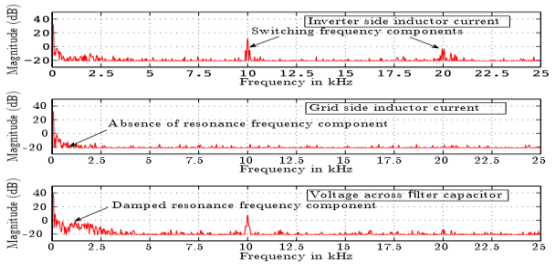

Fig2.2: Spectrum of waveforms in.

A procedure for SC-RL damping circuit design has been proposed with the intent of keeping the QF low in the range of 2.0 to 2.5 and while maintaining the total power loss in the dampingresistor to be in therange of 0.05% to 0.1%. The trade-off involved in systematically designing the passive damping circuit, with choice for C1, Cd and Rd, is provided. A damping impedance factor, KLd, has been introduced in the process of developing the design procedure and is used to select Ld. An expression for a suitable value of KLd is provided. This value of KLd is shown to give a low quality factor along with low losses in the damping resistors. This is verified analytically over a wide range of switching frequencies, power levels and choice of inductance and capacitance values of the filter. The outlined method is useful for high power inverters connected to the grid. Experimental measurements were made using a large number of inductors to vary KLd for practical evaluation of its impact on the filter damping performance.

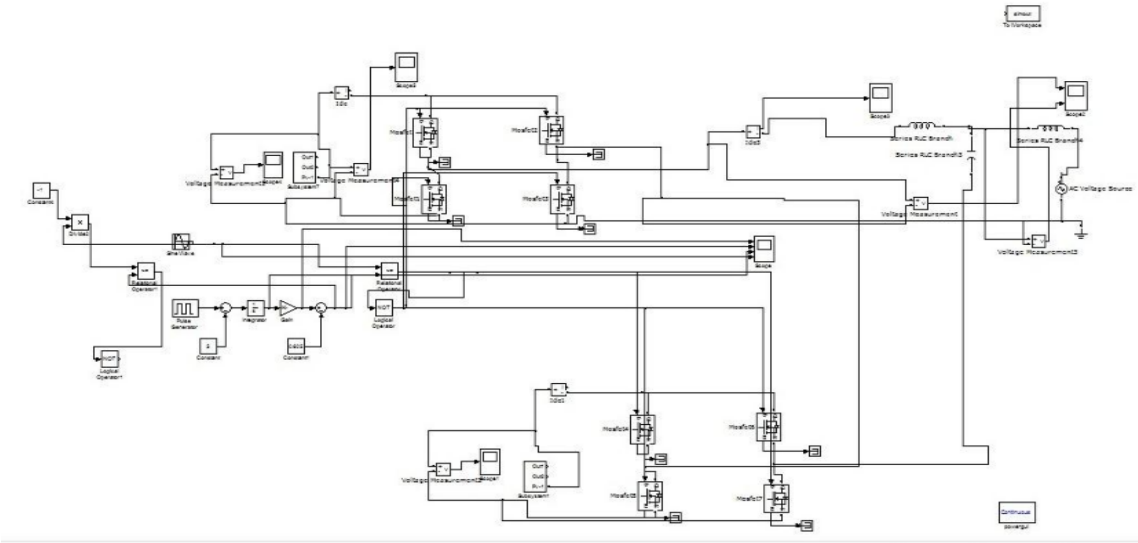

Fig 2.3: grid tied LCL Filter Damping circuit simulation

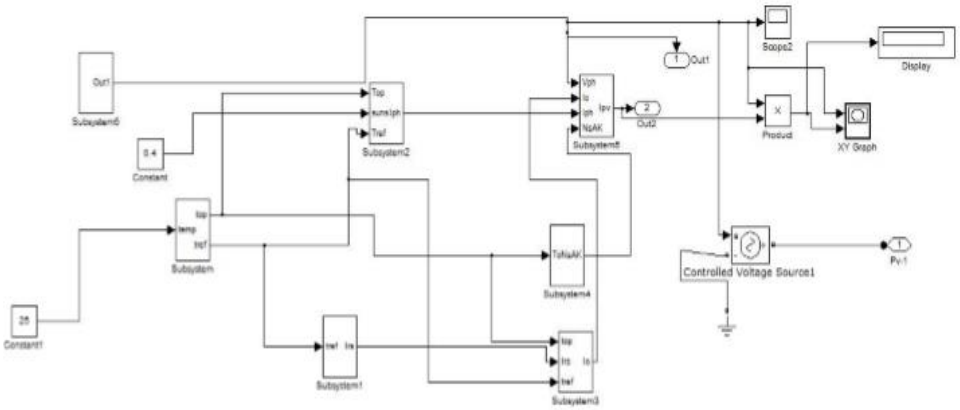

Fig2.4: PV Block Diagram with MPPT

The PV array is simulated in the open circuit case and its characteristics are obtained. The MPPT method used here is found to be more efficient than other MPPT methods and hence better results are obtained using the incremental conductance method. the simulation results obtained of the inverter voltage and PV Array output are as per the system design and are having minimum harmonics.

VII.CONCLUSION

The proposed method aims at reducing the losses in the damping resistor while keeping the system well damped. A component by component optimization and trade-off procedure is used to achieve this. With the proposed method, the power loss in the damping resistor is in the range of 0.05% to 0.1% while the quality factor is in the range of 2.0 to 2.5. The proposed method also

ensures that the additional poles introduced by the passive damping network too are well damped. Further, the method has been shown to be applicable for a wide range of practical switching frequencies. The power loss and quality factor have been verified experimentally to be within the expected range.

REFERENCES

[1] J. M. Carrasco, L. G. Franquelo, J. T. Bialasiewicz, E. Galv´an, R. P. Guisado, M. A. Prats, J. I. Leo´n, and N. Moreno-Alfonso, "Power-electronic systems for the grid integration of renewable energy sources: A survey," IEEE Transactions on Industrial Electronics, vol. 53, no. 4, pp. 1002–1016, 2006.

[2] A. Rockhill, M. Liserre, R. Teodorescu, and P. Rodriguez, "Grid-filter design for a multi-megawatt medium-voltage voltage-source inverter," IEEE Transactions on Industrial Electronics, vol. 58, no. 4, pp. 1205–1217, 2011.

[3] J. Dannehl, F. Fuchs, S. Hansen, and P. Th andgersen, "Investigation of active damping approaches for PI-based current control of grid-connected pulse width modulation converters with LCL filters," IEEE Transactions on Industrial Applications, vol. 46, pp. 1509 –1517, July-August 2010.

[4] Y. Tsuruta and A. Kawamura, "Back to back system for the development and testing of high power DC-DC converter," in Proceedings of 34th Annual Conference of IEEE Industrial Electronics, IECON 2008, pp. 572–577, 2008.

[5] Y. Han, C. Chung, H. Yoo, J. Kim, and S. Kim, "A test facility for large scale inverter valve and pole using resonant circuit," in Proceedings of 7th Internatonal Conference on Power Electronics, 2007. ICPE '07, pp. 548–553, 2007.

[6] J. Chen, C. L. Chu, and C. Huang, "A study on the test of UPS by energy feedback method," in Proceedings of IEEE International Sympoisum on Circuits and Systems, 1991, pp. 3015–3018 vol.5, 1991.

AUTHORS BIOGRAPHY

P. Saravana Kumar received B.E Course from The Rajaas Engineering College Tirunelveli in 2011.M.E[EST] from RVS College of Engineering, Dindigul in 2016 nowResearchscholar of Anna University. His research interests include Embedded System, Power Electronics; Grid tied Inverter and Solar energy

Dr.S. Sutha Padmanabhan received B.E., from government college of Engineering Tirunelveli, monomania Sundarar University in 1996, M.E., from college of Engineering Guindy Anna university Chennai in 2000 and Ph.D., from Anna University Chennai in 2008. Presently; she is working as associate Professor of Anna University (Dindigul Campus) Tamilnadu India.